J Sol-Gel Sci Technol (2017) 83:291–295
DOI 10.1007/s10971-017-4408-x

ORIGINAL PAPER: INDUSTRIAL AND TECHNOLOGICAL APPLICATIONS OF SOL-GEL AND HYBRID MATERIALS

Antireflective coatings by sol–gel processing: commercial products and future perspectives

Peer Löbmann[1]

Received: 7 March 2017 / Accepted: 5 May 2017 / Published online: 13 May 2017

Abstract Commercial antireflective coatings prepared by sol–gel processing are compared to MgF_2 λ/4 thin films. Their respective optical performance is measured by UV-Vis spectroscopy. Microstructural features as characterized by Scanning Electron Microscopy are correlated to results determined by Ellipsometric Porosimetry. A modified Crockmeter testing procedure employing steel wool as abrasive was used to examine mechanical film stability. Results indicate that MgF_2 films can well compete with other porous λ/4 systems, as well as with dense interference multilayer assemblies targeting at superior optical and mechanical properties.

Graphical Abstract The performance of commercially available sol–gel antireflective coatings are compared with porous MgF_2 film system. Results indicate that they exhibit superior properties compared to their SiO_2 counterparts under investigation.

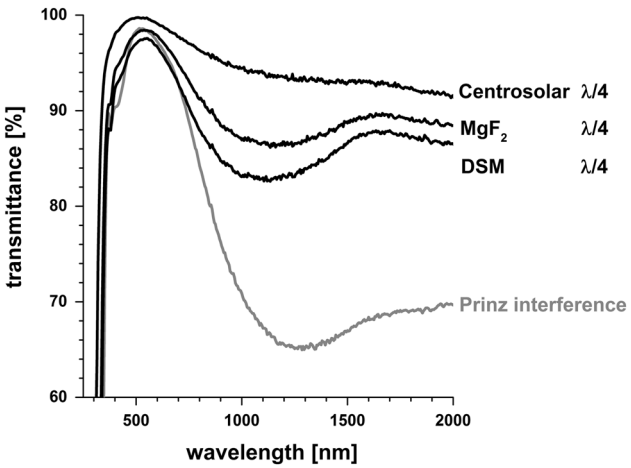

Keywords antireflective coatings · sol-gel · transmittance · porosity · mechanical stability

1 Introduction

Antireflective coatings are of high importance for solar energy conversion, display industry, optical components, ophthalmic lenses, and architectural glazing. Besides vacuum-based technologies the film deposition from liquid precursors has gained considerable scientific and commercial attention: By so-called sol–gel processing different topological approaches such as dense interference layers, porous λ/4 films, and moth-eye structures can be realized [1]. Naturally, any commercial relevance goes along with increasing secretiveness. Industrial products therefore are

✉ Peer Löbmann
peer.loebmann@isc.fraunhofer.de

[1] Fraunhofer-Institut für Silicatforschung, Neunerplatz 2, Würzburg 97082, Germany

hardly ever documented in the scientific literature. Furthermore, it seems that patent applications often are more suitable to nebulize an approach than to disclose technical details. Therefore, it is often difficult to judge the technical relevance of film systems and compositions.

As a result of a publicly funded research project we were able to gain access to some antireflective coatings that are or were commercially available. In this paper the performance of these specimen is compared with porous MgF_2 coatings system that is presently engineered for a future industrial application [2–4].

2 Experimental procedure

2.1 Materials

The 3-layer interference-type antireflective coatings (trade name Pro View green, AR4) were provided by Prinz Optics (Stromberg, Germany). Prinz Optics also used a coating solution based on polymer templates [5–7] originally invented by DSM (DSM, Netherlands) for the fabrication of porous λ/4 antireflective coatings. These films have been commercialized under the trade name "AR 1". Another type of nanoporous SiO_2 λ/4 antireflective films "Hit Float" were supplied by Centrosolar (Fürth, Germany) [8, 9]. Based on precursor solutions [2–4] MgF_2 coatings (λ/4) were produced by Prinz Optics, these systems have not been commercialized yet.

2.2 Characterization

Transmittance curves were measured with an UV-Vis-spectrometer (Shimadzu UV-3100, Kyoto, Japan), in the range of 300–2000 nm.

Cross-sectional views of the films were examined by scanning electron microscopy (SEM), using a Zeiss Ultra 25 (Carl Zeiss SMT, Oberkochen, Germany), Pt was applied prior to the investigation by sputtering.

Thickness, open porosity, and pore radius distribution of the thin films were determined by Ellipsometric porosimetry (EP), (GES 5-E-Ellipsometer Sopra, Paris, France) at room temperature using water vapor as adsorbate [10, 11]. The analysis was performed using the software WinElli II (Version 2.2.0.3, Sopra, Paris, France). The open porosity was measured on the basis of the adsorption and desorption isotherm received by using the Lorentz–Lorenz equation.

The mechanical stability of the films was tested by a custom made Crockmeter-Test using felt and steel wool of the fineness 00 as abrasive. The stamp (contact area 4.5 cm^2) was pressed on the sample with a force of 4 N.

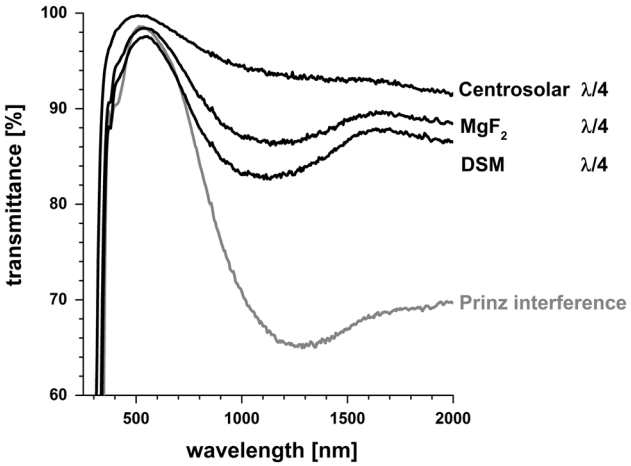

Fig. 1 Transmittance of antireflective coatings under investigation in this study

3 Results and discussion

The transmittance curves of the antireflective coatings under investigation are compiled in Fig. 1. The porous λ/4 SiO_2 antireflective film provided by Centrosolar shows the highest transmittance that exceeds 99 % at a maximum at 500 nm. Second to that the MgF_2 coatings exhibit a maximum >98 % at 550 nm, the bandwidth at higher wavelength is smaller than its SiO_2 counterpart. Both, the maximum transmittance and bandwidth of the DSM systems are smaller than those of MgF_2. The peak transmittance and wavelength of the 3-layer filter by Prinz Optics is close to that of MgF_2, but its bandwidth at higher wavelengths is significantly lower as one would expect from an interference layout compared to λ/4 systems [1].

In Fig. 2 the cross-sectional view of the different antireflective films as derived by SEM are summarized. Even though the interference film of Prinz Optics consists of 3 subsequent coatings [1], only the uppermost low-refractive SiO_2 layer can clearly be distinguished from the underlying TiO_2 and TiO_2/ZrO_2 coatings that exhibit an almost identical microstructure (Fig. 2a).

The single layer antireflective film based on the method invented by DSM [6] shows a completely different microstructure (Fig. 2b): Within the seemingly dense film matrix oval cavities with their longer semiaxis always parallel to the substrate can be seen. Their widest diameter as cut by the fractured surface range from 10 to 80 nm. Since the cavities originate from spherical template particles and the film densification during film annealing only proceeds perpendicular to the substrate, the oval shape of the final pores is consequential. If monodisperse templates are assumed [6], the seeming different size of the cavities results from different intersections through pores with comparable diameters.

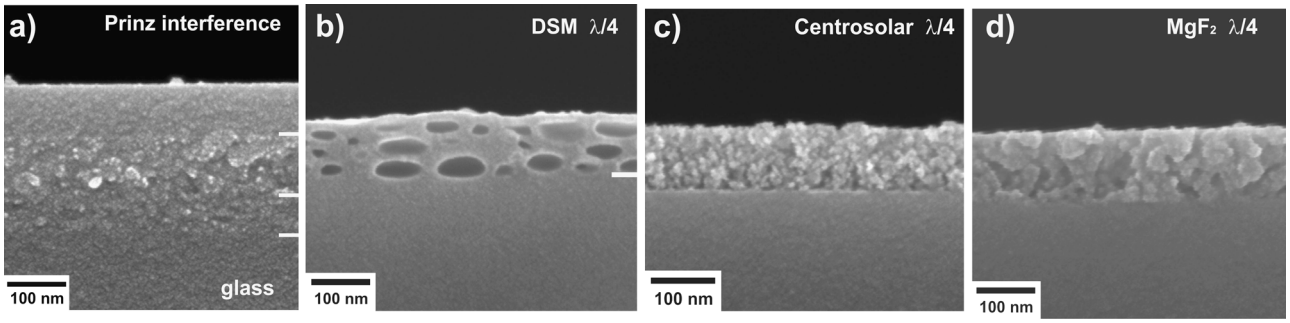

Fig. 2 Cross-sectional SEM images of **a** 3-layer interference filter provided by Prinz Optics, **b** λ/4 layer manufactured based on a coating solution from DSM, **c** SiO_2 λ/4 film manufactured by Centrosolar and **d** MgF_2 λ/4 film

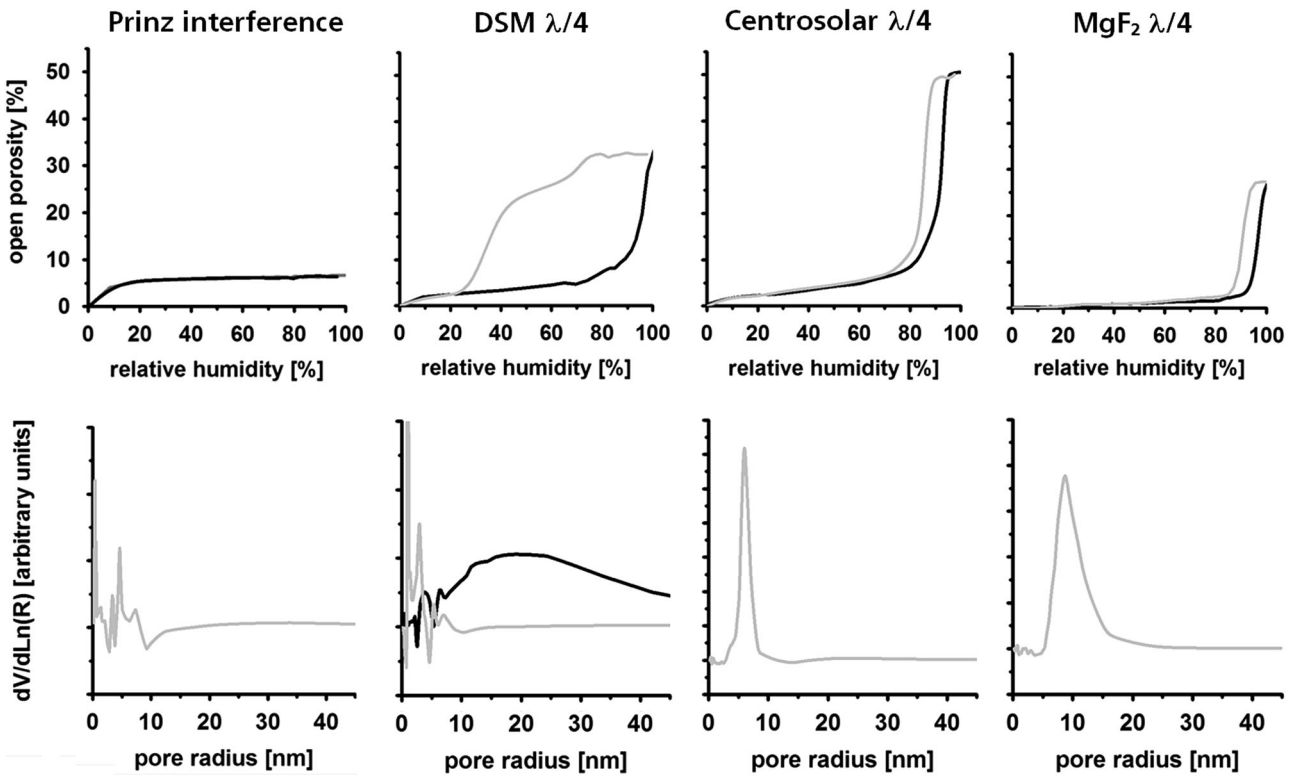

Fig. 3 Sorption isotherms (*upper row*) and derivative pore radius distributions (*lower row*) as measured by EP. The pore radius in general was calculated from the desorption branch (*gray*) of the isotherms, for the DSM λ/4 layer additionally the distribution derived from the adsorptive branch (*black*) is given

The λ/4 SiO_2 film commercialized by Centrosolar (Fig. 2c) exhibits a fine granular constitution, no large cavities are present. The microstructure appears similar to the dense interference assembly. This delusive visual impression demonstrates that the depth of sharpness of SEM imaging prohibits even the semiquantitative analysis of porosity.

The microstructure of the MgF_2 λ/4 coatings (Fig. 2d) is coarser than that of their SiO_2 counterpart (Fig. 2c). Again SEM investigations do not provide any quantitative results regarding film porosity. This topic therefore is addressed by EP.

In the top row of Fig. 3 the water vapor sorption isotherms of the films under investigation as measured by EP are given. Below that, the correspondent derivative pore radius distributions are shown [11]. For all samples the Barrett–Joyner–Halenda (BJH) theory [12] was applied to the desorption branch of the respective isotherms, only for the DSM λ/4 layer additionally also the results derived from the adsorption branch are given.

For the 3-layer interference layer a type-1 isotherm according to the Brunauer, Deming, Deming and Teller theory [13] is observed which is typical for microporous

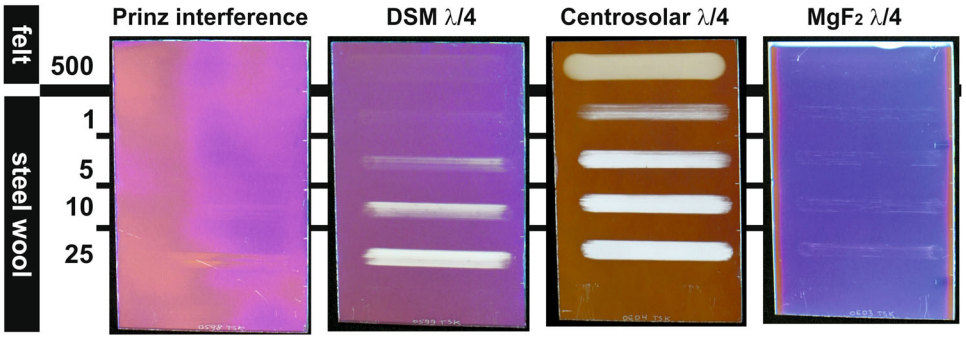

Fig. 4 Photographs of antireflective coatings subjected crockmeter testing using felt (500 cycles) and steel wool (1–25 cycles) as abrasive. The size of the samples shown is 10×15 cm²

Table 1 Film thickness, open porosity, maximum of pore radius distribution, and peak transmittance of antireflective coatings under investigation

Film system	Film thickness [nm]	Open porosity [%]	Max. pore radius [nm]	Peak transmittance [%]	at [nm]
Prinz interference	297	<6	n.a.	98,6	515
DSM λ/4	113	33,2	(19)	97,5	545
Centrosolar λ/4	105	50,2	5,9	99,7	515
MgF_2 λ/4	115	27,3	8,7	98,5	540

systems. A low porosity of approximately 7% is measured, no significant pore radius distribution is obtained by BJH evaluation since this procedure is only valid for pore radii above 2 nm. The microstructure as seen in SEM imaging (Fig. 2a) can be considered comparably dense, a high mechanical stability of these films can be expected.

The sorption curves of the DSM system exhibit a very broad hysteresis. Considering the film microstructure (Fig 2b) this observation can be explained by the so-called inkbottle pores [14]: The access to the large cavities is bounded by a nanogranular structure. These fine pores are filled first before water condensation takes place in the larger voids. Upon decreasing partial pressure the cavities remain filled until the desorption conditions for the small "bottleneck" pores are fulfilled. Then sudden drain from the larger supersaturated volume takes place. As the bottleneck pores are too small to result in a pore radius distribution according to BJH theory, the adsorption isotherm has to be taken for determination of pore radii [15].

The fine granular morphology of the Centrosolar SiO_2 λ/4 layer as seen in Fig. 3c is also reflected in the pore radius distribution showing pores with radii between 5 and 10 nm. With 50% the open porosity is significantly higher than measured for the DSM SiO_2 film (30 %), even though their antireflective properties are comparable (Fig. 1). It has to be noted, though, that the DSM adsorption isotherm does not clearly end in a constant value close to water vapor saturation at $p/p_0 = 1$. It is therefore possible that pores with radii > 50 nm are not accounted for in the DSM film and therefore its total porosity is underestimated.

With radii between 8 and 20 nm the MgF_2 coatings have coarser pores than their Centrosolar counterpart as already suggested by SEM (Fig. 2). As MgF_2 (1,38) has a lower index of refraction than SiO_2 (1,52), good antireflective properties are obtained at a significant lower porosity of 30%.

For any practical application of antireflective coatings, their abrasion resistance is a key factor. In Fig. 4 photographs of the samples under investigation are given after testing. All films withstand 500 cycles with felt as an abrasive, only the porous SiO_2 film by Centrosolar is completely stripped off. In order to further differentiate between the remaining specimen, harsher conditions were applied using steel wool instead of felt.

For the interference antireflective system by Prinz Optics slight marks are observed after 10 and 25 abrasion cycles with steel wool. This high damage resistance results from the dense microstructure of the multilayer assembly.

For the DSM film an increasing damage takes place, after 25 cycles the film is completely removed. It can be envisioned that if the upper film surface is damaged and some of the large pores become exposed, these excavations are successively enlarged by the steel wool abrasive and irregular film fragments. Originating from such surface damages lower regions of the film become harmed until finally the complete material is removed from the substrate.

In the case of MgF_2 λ/4 layers only a minor damage is visible that does not significantly increased with the number of cycles. Obviously, the porous MgF_2 material (30% porosity) better withstand the abrasive wear than its SiO_2 equivalent with 50% porosity.

In Table 1 the properties of the films under investigation are compiled. The respective thickness was derived from the SEM images (Fig. 2). Open porosity and maximum of pore radius distribution originate from the EP data of Fig. 3,

whereas the transmittance is taken from Fig.1. For the Prinz interference filter no reliable open poosity could be measured, therefore an upper limit of 6% is assumed. As the DSM films exhibit inkbottle pores the maximum corresponding to the large cavities (analysis of the adsorption branch) is given.

4 Conclusions

Sol–gel derived from dense interference antireflective coatings provide good mechanical properties, their optical bandwidth is rather limited, though. Amongst porous λ/4 systems the novel MgF_2 films exhibit superior mechanical film stability compared to their SiO_2 counterparts under investigation.

Acknowledgements We are grateful to Prinz Optics (Stromberg, Germany) for providing commercial samples and performing coating experiments. The author thanks the research group of Erhard Kemnitz at the Humboldt University, Berlin, for the supply of MgF_2 coating solutions. This project was funded by the German Federal Ministry of Economic Affairs and Energy (Grant 03ET1235A).

Compliance with ethical standards

Conflict of interest The author declare that he has no competing interest.

References

1. Löbmann P (2013) Antireflective coatings and optical filters. In: Schneller T, Waser R, Kosec M, Payne D (Eds.) Chemical solution deposition of functional oxide thin film. Springer, Wien, Heidelberg, New York, NY, p 707–724
2. Noack J, Scheurell K, Kemnitz E, Garcia-Juan P, Rau H, Lacroix M, Eicher J, Lintner B, Sontheimer T, Hofmann T, Hegmann J, Jahn R, Löbmann P (2012) MgF_2 antireflective coatings by sol-gel processing: film preparation and thermal densification. J Mat Chem 22:18535–18541
3. Scheurell K, Noack J, König R, Hegmann J, Jahn R, Hofmann T, Löbmann P, Lintner B, Garcia-Juan P, Eicher J, Kemnitz E (2015) Optimisation of a sol–gel synthesis route for the preparation of MgF_2 particles for a large scale coating process. Dalton Trans 44:19501–19508
4. Scheurell K, Kemnitz E, Garcia-Juan P, Eicher J, Lintner B, Hegmann J, Jahn R, Hofmann T, Löbmann P (2015) Porous MgF_2 antireflective λ/4 films prepared by sol–gel processing: comparison of synthesis approaches. J Sol-Gel Sci Technol 76:82–89
5. Arfsten N, Buskens P, Habets R. Inorganic Oxide Coating. WO 2011157820
6. Boerakker M, Buskens P, Armes S, Arfsten N (2011) Optische effecten door holle nanodelen. Nederlands Tijdschrift voor Natuurkunde 6:227–229
7. Arfsten N, VanDijck M, Dabets R. Composition and Process for Making a Porous Inorganic Oxide Coating. WO 2013174754
8. Glaubitt W, Kursawe M, Gombert A, Hofmann T. Glass Comprising a Porous Anti-Reflective Surface And Method For Producing One Such Glass. WO03/027034
9. Ballif C, Dicker J, Borchert D, Hofmann T (2004) Solar glass with industrial porous SiO_2 antireflection coating: measurements of photovoltaic module properties improvement and modelling of yearly energy yield gain. Sol Energy Mat Sol Cells 82:331–344
10. Baklanov MR, Mogilnikov KP, Polovinkin VG, Dultsev FN (2000) Determination of pore size distribution in thin films by ellipsometric porosimetry. J Vac Sci Technol B 18(3):1385–1391
11. Baklanov M, Green M, Maex K (2007) Dielectric films for advanced microelectronics. Wiley, West Sussex
12. Gregg SJ, Sing KSW (1982) Adsorption, surface area and porosity, 2nd edn. Academic Press, London
13. Brunauer S, Deming L, Deming W, Teller E (1940) On a theory of the van der Waals adsorption of gases. J Am Chem Soc 62:1723–1732
14. Casanova F, Chiang C, Li C, Schuller I (2007) Direct observation of cooperative effects in capillary condensation: the hysteretic origin. Appl Phys Lett 91:243103
15. Gidley D, Peng H, Vallery R, Soles C, Lee H, Vogt B, Lin E, Wu W, BaklanovM (2007) Porosity of low dielectric constant material. In: Baklanov M, Green M, Maex K (Eds.) Dielectric films for advanced microelectronics. John Wiley & Sons, Chichester, UK, p 85–136.